Uniformly Converging Schemes for Discontinuous Seismic Wave Problems

H. Munthe-Kaas* D. Eke*

June 1996

Abstract

In numerical modeling of elastic wave propagation, standard numerical simulation schemes suffer from numerical errors, in the form of Gibbs oscillations, caused by discontinuities in material properties. A new modification scheme to the standard differentiation operator aimed at reducing these errors is proposed. It is based on computing derivative correction factors from analytical and numerical derivatives of a special test function. This modification scheme can be applied to virtually any differentiation scheme and on complicated models. A pseudospectral algorithm using this technique is presented.

1 Introduction

There has been a growing interest in the oil and natural gas exploration industry for a better and more reliable interpretation of seismic surveys (data) obtained from exploration seismology. *Forward modeling* - a term used to describe the simulation of seismic waves propagating in a model with known material properties - provides the synthetic results which are compared to the recorded data for geological interpretation and model verification. Forward modeling involves the direct solution of a mathematical model in the form of elastic wave equations which relate the response of the subsurface (geological structure) to the seismic excitation.

Increased research interest has been directed therefore, to designing accurate numerical methods for simulating elastic wave propagation within a realistic model that retains most of the geological meaningful features. These methods include finite differences (e. g. Holberg [1], Squazzero et al. [2], Mora [3]), finite elements (e. g. Priolo and Seriani [4]) and pseudospectral (Fourier) methods (e. g. Berg [5], Berg et al. [6], Reshef et al. [7], Kosloff et al. [8]). These methods share the advantage of the ability to handle complete material variability. However, one major disadvantage has been the errors introduced by inaccurate approximation of the spatial derivatives in the wave equations. Because of the material variability, the wave variables - displacement, stress and acceleration - exhibit finite regularity and are therefore not infinitely differentiable. In fact, these variables at the material interfaces are only regular to the first degree (exist on C^0 space). That means that these functions are not differentiable at the interfaces. Numerical differential operators, therefore, produce spurious oscillations (popularly referred to as Gibbs phenomenon) in a region around the interface.

*Dept. of Informatics, University of Bergen, Norway

Several numerical algorithms to deal with this problem have been proposed. Filho [9] introduced the dual operator scheme in his finite difference forward modeling scheme in which a short operator is used to differentiate material variables and a long operator to differentiate the displacement field. Fornberg [10] proposed a method where curved discontinuity lines are transformed into straight horizontal lines. A relatively easier technique in implementation was suggested by Muir et al. [11] in which averaging techniques are employed to modify material properties near the discontinuities.

In this work, we present a new approach - *test function approach* - based on modifying standard differentiation operators. The basic idea is to construct a special test function with a known analytical derivative. From the numerical and analytical results, correction factors that effectively remove Gibbs oscillations are computed. The implementation of the technique using pseudospectral method in which the spatial derivatives are approximated using our modification scheme on the Fourier derivative operator is described. The temporal derivatives are computed using the standard center-difference scheme. Illustrative examples using our scheme for simple two-dimensional (2D) elastic simulations are presented.

2 Elastic Wave Equations

The propagation of waves in an elastic medium is governed by the elastic properties of the underlying materials and the conservation of momentum. The general theory of elasticity describing the mechanics of motion and deformation of an elastic material coupled with the corresponding equations that relate stress and strain for a linearly elastic material - *Hooke's law* - are the tools used in obtaining the equations that describe the motion and deformation of elastic materials in response to applied forces. We consider here a vertical 2-D medium with a horizontal axis x going from left to right and a vertical axis z pointing downwards. The medium is linearly elastic and isotropic.

The two dimensional equations of motion that define wave propagation in elastic medium are given by [12]:

$$\rho\frac{\partial^2 u_x}{\partial^2 t} = \frac{\partial\sigma_{xx}}{\partial x} + \frac{\partial\sigma_{xz}}{\partial z} + s_x \tag{1}$$

$$\rho\frac{\partial^2 u_z}{\partial^2 t} = \frac{\partial\sigma_{xz}}{\partial x} + \frac{\partial\sigma_{zz}}{\partial z} + s_z \tag{2}$$

Hooke's law - which relates stresses to the changes in shapes and dimensions of our medium (strain) - supplements the equations (1) and (2):

$$\sigma_{xx} = (\lambda + 2\mu)e_{xx} + \lambda e_{zz} \tag{3}$$

$$\sigma_{xz} = 2\mu e_{xz} \tag{4}$$

$$\sigma_{zz} = \lambda e_{xx} + (\lambda + 2\mu)e_{zz} \tag{5}$$

where

$$e_{xx} = \frac{\partial u_x}{\partial x} \tag{6}$$

$$e_{xz} = \frac{1}{2}\left(\frac{\partial u_z}{\partial x} + \frac{\partial u_x}{\partial z}\right) \tag{7}$$

$$e_{zz} = \frac{\partial u_z}{\partial z} \tag{8}$$

Here σ_{xx}, σ_{zz} and σ_{xz} are stress components and e_{xx}, e_{zz} and e_{xz} are the corresponding strain components. u_x and u_z are the displacements in the x and z directions respectively. The coefficients λ and μ are the Lames parameters, ρ is the density and s_x and s_z are the applied body forces that generate the disturbance. We shall look into these forces in the next section.

The material parameters λ, μ and ρ of the medium determine the propagation of the disturbance generated by s_x and s_z. For an isotropic medium, only these parameters describe the elastic material. In forward modeling, these are assumed known functions of the spatial coordinates x and z.

The isotropic medium supports two major types of waves : *compressional waves* known as P-waves and *shear waves* known as S-waves traveling with different velocities. The material parameters ρ, λ, μ determine the velocities of these two major waves:

$$c_p = \sqrt{\frac{\lambda + 2\mu}{\rho}}, \; c_s = \sqrt{\frac{\mu}{\rho}} \tag{9}$$

where c_p and c_s are P-wave and S-wave velocities respectively. The compressional part of the wave field, P, is the divergence of the displacement vector:

$$P = -(\lambda + 2\mu)(\frac{\partial u_x}{\partial x} + \frac{\partial u_z}{\partial z}) = \frac{1}{2}(\sigma_{xx} + \sigma_{zz}) \tag{10}$$

while the rotational part, S, is the curl of the displacement vector:

$$S = \mu(\frac{\partial u_x}{\partial z} - \frac{\partial u_z}{\partial x}) \tag{11}$$

The source terms (s_x, s_z) used in this work are localized body forces:

$$\begin{aligned} s_x(x,z,t) &= \frac{\partial f(x,z)}{\partial x} h(t) \\ s_z(x,z,t) &= \frac{\partial f(x,z)}{\partial z} h(t) \end{aligned}$$

where $f(x,z)$ is a scalar function localized around a source position (x_s, z_s) and $h(t)$ is a 2-loop ricker wavelet time history, see Fig. 1(left).

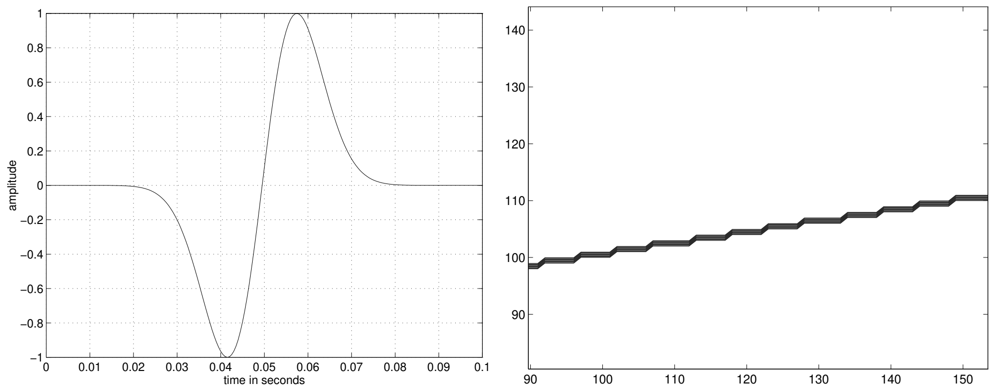

Figure 1: *A 2-loop ricker wavelet time history with peak frequency $f_p = 20hz$ and time delay 50 msec (left) and staircase representation of plane dipping interface (right)*

2.1 The Discontinuity Problem

2.1.1 Gibbs Phenomenon

In a heterogeneous medium, the Lamé's parameters $\lambda(x,z)$ and $\mu(x,z)$, and the material density $\rho(x,z)$ in the elastic wave equations are discontinuous across the material interface border. The displacement vector $u(x,z,t)$, stress tensor $\sigma(x,z,t)$ and acceleration $\partial^2 u/\partial^2 t$ are continuous to the first degree. This implies that u and σ are C^0-continuous across the material interface, i. e. they are continuous with discontinuous derivatives.

The analytical solution u to the elastic wave equation is in the space C^0; therefore its approximations will be highly oscillatory, with the oscillations particularly bad close to the discontinuity - *Gibbs phenomenon*. Because of the Gibbs phenomenon, neither spectral differentiation nor finite differences to u and σ will converge uniformly; the methods will always produce oscillatory errors of significant heights near the discontinuities, regardless of grid size.

2.1.2 Grid Diffraction

In numerical modeling of elastic wave propagation, the geological model is defined by assigning values for the elastic materials at every grid point. The discrete grid is not able to sense the exact position of the discontinuities between the grid nodes other than between nearest grid points with different values of the elastic parameters. Curved and dipping interfaces will, therefore, translate to staircase curves on the rectangular grid (artificial corners), see fig. 1(right). This causes diffractions from these artificial corners. Fornberg's mapping approach in which curved interfaces are transformed into straight horizontal lines work well for very simple geometries. It is known that horizontal interfaces produce very small errors during differentiation and pose little diffraction problems. This approach is, unfortunately, very difficult to implement for realistic geometries. Schoenberg-Muir approach uses certain averaging techniques to evaluate equivalent material parameters for the grid cells containing the interfaces. This approach is known to smooth out the discontinuity, thereby reducing grid diffraction. A major disadvantage however, is that equivalent medium becomes anisotropic even though the original medium is isotropic. The approach by Filho does not solve the Gibbs phenomenon problem since the method uses a (long) standard operator to differentiate u and σ.

In the next section, we present our new approach (which we call a *a test function approach*) to improve differentiation over discontinuities in elastic wave modeling. It utilizes information on the exact positions of the discontinuities, hence will reduce also the grid diffraction problem.

3 Test Function Approach

This approach is based on constructing a modified numerical differential operator ∂^* based on the standard operator $\hat{\partial}$ which converges uniformly for $\gamma\partial\psi$, where γ and $\partial\psi$ satisfy certain properties. The idea is to probe Gibbs errors by numerically differentiating a special test function with a known analytical derivative [17]. Correction factors to the standard numerical differential operator that effectively remove the Gibbs oscillations are computed from the numerical and analytical results.

We present next the basic assumptions we have made in the formulation of our scheme.

Assumptions:

1. The function ψ is continuous in an open interval $\Omega \subset R$.
2. γ is a piecewise continuous function with discontinuities at the points $\{x_i\}_{i=1}^{N} \epsilon\, \Omega$.
3. ψ exists, except at $\{x_i\}$, and $\gamma\partial\psi$ is Lipschitz continuous:

$$|(\gamma\partial\psi)(x+\Delta x) - \gamma\partial\psi(x)| \leq L\,|\Delta x|\,,\ \forall x, \Delta x$$

   where L is the Lipshitz constant.
4. Let $\hat{\partial}$ be standard numerical differential operator and h the discretization parameter:
   - $\hat{\partial}$ is linear
   - $\hat{\partial}$ converges uniformly for all C^1 functions:

$$\left|\hat{\partial} f(x) - \partial f(x)\right| \leq c_u h$$

     where $f(x) \epsilon C^1$, c_u is a constant independent of x but on f.
   - $\hat{\partial}$ converges pointwise at all points where $f(x) \epsilon C^1$ in a neighborhood containing x:

$$\left|\hat{\partial} f(x) - \partial f(x)\right| \leq c_p(x) h.$$

     where c_p depends on x and f.
5. $|x|\hat{\partial}|x|$ converges uniformly $\forall\, x \,\epsilon\, R\backslash\,\{0\}$. This implies:

$$\left||x|\hat{\partial}|x| - |x|\partial|x|\right| \leq c_u h. \tag{12}$$

   This assumption is valid for finite-difference and spectral differential operators. For most methods $c_u \lesssim 1$.

Theorem 3.1 *Define the operator ∂^* by:*

$$\partial^*\psi = \frac{\hat{\partial}\psi}{1 - \gamma(\hat{\partial}\tau - \partial\tau)}$$

where τ is a special test function defined by equations(13)–(15).
Let Ω be an interval where

$$\left|\hat{\partial}\psi\right| \geq K > 0 \; and \; \partial\psi \neq 0$$

$\forall x \,\epsilon\, \Omega$ (K is independent of x).
Then $\gamma\partial^*\psi$ converges uniformly to $\gamma\partial\psi$ in Ω:

$$|\gamma\partial^*\psi - \gamma\partial\psi| \leq Ch\,|\gamma\partial^*\psi|$$

$\forall x \,\epsilon\, \Omega$, where

$$C = \sum_{i=1}^{N} \frac{1}{2}\left|\frac{1}{\gamma_+(x_i)} - \frac{1}{\gamma_-(x_i)}\right| \frac{Lc_u}{K} + \frac{c'}{K}.$$

and c' is a constant independent of x, L is the Lipschitz constant of $\gamma\psi$, and c_u is the uniform bound in equation (12).

As would be expected, the most influential of the discontinuities is the closest so that we can approximate C:

$$C = \frac{1}{2}\left|\frac{1}{\gamma_+} - \frac{1}{\gamma_-}\right|\frac{Lc_u}{K} + \frac{c'}{K}.$$

The test function $\tau(x)$ in the above theorem is a piecewise polynomial of second degree except at the discontinuities $\{x_i\}_{i=1}^N$. This means that $\tau(x) \epsilon C^0$ which is in harmony with our displacement and stress variables of our elastic wave equations.

The test function $\tau(x)$ is constructed as follows:

$$\partial_- \tau(x_i) = -\frac{1}{2}\left(\frac{1}{\gamma_-(x_i)} - \frac{1}{\gamma_+(x_i)}\right), \tag{13}$$

$$\partial_+ \tau(x_i) = +\frac{1}{2}\left(\frac{1}{\gamma_-(x_i)} - \frac{1}{\gamma_+(x_i)}\right) \tag{14}$$

We choose $\tau(0) = 0.0$.

$\tau(x)$ as defined above is uniquely defined up to additive constant. The constants are chosen such that:

$$\tau(x) = \sum_{i=1}^{N} \tau_i(x) \tag{15}$$

which therefore defines τ uniquely in Ω, since $\tau(x)$ is continuous.

Before proving the above theorem, we introduce the following lemma that is central in the proof of the theorem.

Lemma 3.1 *The function*

$$\tilde{\psi}(x) = \psi(x) + \sum_i \gamma_- \partial_- \psi(x_i)\tau_i(x)$$

is a C^1 *continuous function* $\forall\, x$.

Proof Lemma: ψ and $\tau_i \,\epsilon\, C^0 \Rightarrow \tilde{\psi} \,\epsilon\, C^0$.
For all $x \neq x_i$, ψ and $\tau_i \,\epsilon\, C^1 \Rightarrow \psi \,\epsilon\, C^1$ outside the discontinuities.

$$\begin{aligned}
\partial_- \tilde{\psi}(x_i) &= \partial_- \psi(x_i) + \sum_j \gamma_- \partial_- \psi(x_j)\partial_- \tau_j(x_i) \\
&= \partial_- \psi(x_i) + \gamma_- \partial_- \psi(x_i)\partial_- \tau_i(x_i) \\
&= \partial_- \psi + \gamma_- \partial_- \psi \frac{1}{2}\left(\frac{1}{\gamma_+} - \frac{1}{\gamma_-}\right) \\
&= \partial_- \psi + \partial_- \psi \frac{1}{2}\left(\frac{\gamma_-}{\gamma_+} - 1\right)
\end{aligned}$$

Since

$$\gamma_- \partial_- \psi = \gamma_+ \partial_+ \psi \Rightarrow \frac{\gamma_-}{\gamma_+} = \frac{\partial_+ \psi}{\partial_- \psi}$$

then

$$\begin{aligned}
&\partial_- \tilde{\psi}(x_i) = \\
&\quad \partial_- \psi + \partial_- \psi \frac{1}{2}\left(\frac{\partial_+ \psi}{\partial_- \psi} - 1\right) = \\
&\quad \frac{1}{2}(\partial_+ \psi + \partial_- \psi).
\end{aligned}$$

Correspondingly

$$\partial_+\tilde{\psi}(x_i) = \frac{1}{2}(\partial_+\psi(x_i) + \partial_-\psi(x_i)) = \partial_-\tilde{\psi}(x_i). \bullet$$

Proof Theorem: From lemma (3.1), we showed that $\tilde{\psi} \,\epsilon\, C^1$, and hence converges uniformly:

$$\begin{aligned}\left|\hat{\partial}\tilde{\psi} - \partial\tilde{\psi}\right| &\leq C_\psi h \\ &\Downarrow \\ \partial\psi + \sum_i \gamma_-\partial_-\psi(x_i)\partial\tau_i(x) &= \\ \hat{\partial}\psi + \sum_i \gamma_-\partial_-\psi(x_i)\hat{\partial}\tau_i(x) + ch\end{aligned}$$

where $|c| \leq C_\psi$.

$$\partial\psi = \hat{\partial}\psi + \sum_i \gamma_-\partial_-\psi(x_i)(\hat{\partial}\tau_i - \partial\tau_i) + ch$$

Since $\gamma\partial\psi(x)$ is Lipschitz continuous, we have:

$$\begin{aligned}&\partial\psi = \\ &\quad \hat{\partial}\psi + \gamma(x)\partial\psi(x)\sum_i(\hat{\partial}\tau_i - \partial\tau_i) + \\ &\quad l\sum_i |x - x_i| (\hat{\partial}\tau_i - \partial\tau_i) + ch\end{aligned}$$

where $|l| \leq L$ and L is the Lipschitz of $\gamma\partial\psi$.

$$\begin{aligned}\partial\psi &= \hat{\partial}\psi + \gamma\partial\psi(\hat{\partial}\tau - \partial\tau) + \\ &\quad l\sum_{i=1}^{N} |x - x_i| (\hat{\partial}\tau_i - \partial\tau_i) + ch \\ &\Downarrow \\ \partial\psi &= \frac{\hat{\partial}\psi}{1 - \gamma(\hat{\partial}\tau - \partial\tau)} + \\ &\quad \frac{l\sum_{i=1}^{N} |x - x_i| (\hat{\partial}\tau_i - \partial\tau_i) + ch}{1 - \gamma(\hat{\partial}\tau - \partial\tau)}\end{aligned}$$

Noting that

$$\tau_i(x) = \frac{1}{2}(\frac{1}{\gamma_-} - \frac{1}{\gamma_+})\,|x - x_i| + g(x),$$

where $g(x) \,\epsilon\, C^1$, we obtain:

$$\begin{aligned}\hat{\partial}\tau_i - \partial\tau_i &= \frac{1}{2}(\frac{1}{\gamma_-} - \frac{1}{\gamma_+})(\hat{\partial}\,|x - x_i| \\ &\quad - \partial\,|x - x_i|) + c'h\end{aligned}$$

where c' is independent of x.
From assumption (5), we deduce

$$|x - x_i|\,(\hat{\partial}\,|x - x_i| - \partial\,|x - x_i|) \leq c_u h$$

which gives:

$$l \sum_{i=1}^{N} |x - x_i| \left(\hat{\partial}\tau_i - \partial\tau_i\right) \leq l c_u \sum_{i=1}^{N} \frac{1}{2} \left| \frac{1}{\gamma_+} - \frac{1}{\gamma_-} \right| h.$$

Hence

$$\partial\psi = \partial^*\psi + \frac{l c_u \sum_i \frac{1}{2} \left| \frac{1}{\gamma_+} - \frac{1}{\gamma_-} \right| h + c' h}{1 - \gamma(\hat{\partial}\tau - \partial\tau)}.$$

This proves uniform convergence as long as the factor $1 - \gamma(\hat{\partial}\tau - \partial\tau)$ is limited and away from 0.
Since

$$1 - \gamma(\hat{\partial}\tau - \partial\tau) = \frac{\hat{\partial}\psi}{\partial^*\psi}$$

we obtain:

$$\left| \frac{\gamma\partial\psi - \gamma\partial^*\psi}{\gamma\partial^*\psi} \right| \leq \frac{l c_u \frac{1}{2} \sum_{i=1}^{N} \left| \frac{1}{\gamma_+(x_i)} - \frac{1}{\gamma_-(x_i)} \right| h + c' h}{\min x \left| \hat{\partial}\psi(x) \right|} \bullet$$

The correction factors are given by:

$$\frac{1}{1 - \gamma(\hat{\partial}\tau - \partial\tau)}$$

From the analysis above the following results are proven:

- The corrected scheme
$$\partial^*\psi = \frac{\hat{\partial}\psi}{1 - \gamma(\hat{\partial}\tau - \partial\tau)}$$
converges uniformly as $\mathcal{O}(h)$ under very general assumptions; e. g. the correction scheme works for any spectral and finite difference derivation scheme.

- At distances away from the discontinuities where there is no difference in τ, $\hat{\partial}\tau - \partial\tau = 0$; which implies that the corrected schemes converge pointwise just as their uncorrected counterparts in smooth regions.

The elastic wave equations (1)–(8) can be reformulated as:

$$\begin{aligned}
\frac{\partial^2 u_x}{\partial^2 t} &= \frac{1}{\rho}\frac{\partial}{\partial x}\left((\lambda + 2\mu)\frac{\partial u_x}{\partial x} + \lambda\frac{\partial u_z}{\partial z}\right) + \\
&\quad \frac{1}{\rho}\frac{\partial}{\partial z}\left(\mu\frac{\partial u_z}{\partial x} + \mu\frac{\partial u_x}{\partial z}\right) + \frac{1}{\rho}s_x \\
\frac{\partial^2 u_z}{\partial^2 t} &= \frac{1}{\rho}\frac{\partial}{\partial x}\left(\mu\frac{\partial u_z}{\partial x} + \mu\frac{\partial u_x}{\partial z}\right) + \\
&\quad \frac{1}{\rho}\frac{\partial}{\partial z}\left(\lambda\frac{\partial u_x}{\partial x} + (\lambda + 2\mu)\frac{\partial u_z}{\partial z}\right) + \frac{1}{\rho}s_z
\end{aligned}$$

in which we recognize our Lipschitz continuous functions $\gamma\partial\psi$ as stresses and accelerations.

Our test function approach can therefore be summarized as follows:

1. Based on the material data, $1/\rho, \lambda$ and μ, compute test function for each spatial direction.
2. Compute the derivatives of the test function using the standard numerical differential scheme. Compute the errors and find correction factors. One correction factor for each grid point for x and y derivatives respectively is computed.
3. In the time integration, each partial derivation is succeeded by a pointwise multiplication of the derivative with the correction factors.

The correction factors are time independent, hence are pre-computed. The additional cost of this algorithm to the standard scheme is, therefore, marginal.

4 Numerical Method

In this work, we have implemented our correction scheme using the pseudospectral (Fourier) semi-discretization scheme. The Fourier method consists of replacing the space derivatives in the elastic wave equations over a uniform grid by the analytical derivative of the interpolating trigonometric polynomial over the grid points. This leads to a system of differential-difference equations which can be solved numerically by any suitable integration scheme.

4.1 Space Derivatives

Define the grid points with uniform spacing h:

$$\begin{aligned} x_i &= x_0 + (i-1)h,\ i = 1, 2, \ldots, N \\ z_j &= z_0 + (j-1)h,\ j = 1, 2, \ldots, N \end{aligned}$$

the space derivatives in our model elastic wave equations are computed as follows: given the variable values at the defined grid points, the x-derivatives for each grid line $z = z_j$ are obtained by carrying out a forward FFT in the x-direction. The results are then multiplied by $(2\pi ik/hN)$ the horizontal wave numbers and then an inverse FFT back to the physical space yields the x-derivative at all the points $x = x_i$. Correction is made by pointwise multiplication of the derivative by the correction factors. The same procedure is also carried out for the z-derivatives.

4.1.1 Absorbing Boundaries

Calculation of spatial derivatives using FFT algorithm implies periodic boundary conditions which is not in agreement with our seismic wave propagation problem. This assumed periodicity gives rise to the so-called *wraparound*: waves passing one of the grid boundaries re-enter the computational area via the opposite grid boundary. This eventually destroys the wave field under study. Solution to this problem involves the use of absorbing boundaries. In this work, we have implemented the method suggested by Cerjan et al. [13].

$$G = \exp(-(\gamma(N-i))^2) \tag{16}$$

An absorbing region is created around the grid boundaries. After each time step, the values of the wave amplitude (displacement and displacement derivatives) are multiplied by a smooth gaussian damping function G, which reduces their values at these absorbing regions; subsequently reducing its wraparound effects in the model area where signals are recorded, see Fig. 2.

This scheme can be improved by reducing the velocity of the wave field in the absorbing region by multiplying it with a damping function H:

$$H = \exp(-(\gamma\prime(N-i))^2)$$

This makes the wave to spend more time in this region, thereby increasing the effect of the damping function G [16].

Differences in *Acoustic Impedance* - the product of density and seismic velocity - normally provide the reflecting horizons in seismic wave propagation. Therefore, the reduction of the velocity as recommended above results in new reflections at the absorbing interface. This can be remedied by correspondingly increasing the density at the absorbing layer to keep the acoustic impedance constant in this region. In the initialization phase therefore, the velocities v_p and v_s are multiplied by H and the density ρ is divided by H, hence maintaining a constant acoustic impedance in the absorbing region:

$$\tilde{v_p} = v_p H,\ \tilde{v_s} = v_s H,\ \tilde{\rho} = \rho / H$$

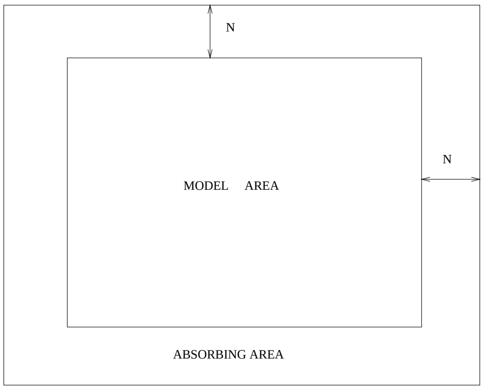

Figure 2: *Model configuration showing the model area and the absorbing area.*

4.2 Time Integration

Several research work has been directed towards designing the most effective time integration scheme that will utilize the high accuracy of the pseudospectral scheme. Recent algorithm is the spectrally accurate time scheme initiated by Tal Ezer [14] in which the evolution operator is expanded by using Chebyshev expansion series. The advantage of this time integration algorithm is that the numerical scheme is unconditionally stable. However, more computational work is performed at each time step compared to approximation of the evolution operator by standard finite difference schemes. In this work, we have used the standard finite difference approximation to the second order time derivative of our wave equation:

$$\ddot{\psi}(t) \approx \frac{\psi(t+\Delta t) + \psi(t-\Delta t) - 2\psi(t)}{(\Delta t)^2} + \mathcal{O}(\Delta t^2)$$

4.3 Stability Conditions

Pseudospectral scheme is essentially a non-dispersive algorithm. Consequently, the only limitation on the size of grid spacing we have used in our implementation is that it fulfills the Nyquist Criteria:

$$\Delta x, \Delta z \leq \frac{c_{min}}{2 f_{max}}$$

where $\Delta x, \Delta z$ are grid spacing in x and z directions respectively, c_{min} is the minimum wave velocity in the model and f_{max} is the maximum frequency of the source time history.

The stability condition for the central second order time integration scheme used in this work, is that given by Kosloff et al. [15]:

$$\Delta t \leq \frac{\sqrt{2}\min(\Delta x, \Delta z)}{2\pi c_{max}}$$

where c_{max} is the maximum wave velocity of the model.

5 Numerical Experiments

To illustrate forward modeling with the new modification technique on the spatial differential operator, we consider wave propagation in a simple horizontal layer model and a dipping interface model. Analytical solutions to the horizontal and dipping interface models are available and will be compared to the numerical solutions.

In all the examples, we have used a source with a two-loop ricker wavelet time history (fig. 1) with peak frequency $f_p = 20Hz$ and delay $t_0 = 50ms$. The size of all models is $256x256$, with grid size $\Delta x = \Delta z = 8.0m$. The propagation is carried up to $0.4s$ with a time increment of $0.5msec$. We have not implemented any free surface condition. All test programs are written in $MATLAB$.

5.1 Horizontal layer model

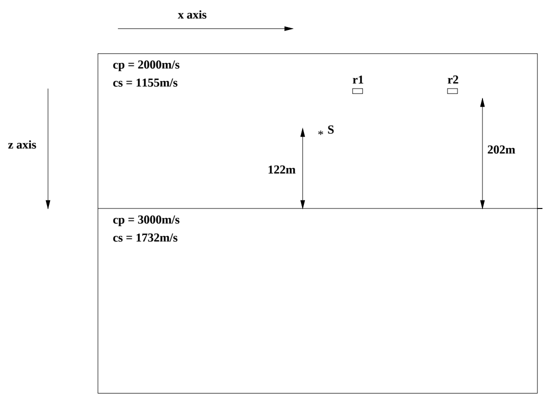

Figure 3: Configuration of horizontal layer model. (S) source, (r1, r2) receivers.

The configuration of the model is shown in fig 3. The model consists of two solid half-space with uniform density. The source is applied at the center of the model at a height of $122m$

above the interface. The receivers are placed at a height of $202m$ above the interface, and are $80m$ away from each other and the source for the first receiver.

In figures (4) - (7), we show the time series of horizontal and vertical displacements at receiver positions for our modified and standard algorithms in dotted lines. The semi-analytic solutions obtained by ray-tracing technique are shown in bold lines.

The first arrivals are the direct wves from the source. Later (at $t > 0.2s$), the interface reflected waves arrive. It is clearly seen that the interface reflected waves are in better agreement with the semi-analytic solutions for our modified scheme. The direct wave, as expected, is same for the standard and modified algorithms.

Even though the geometry of this example is simple, it poses a considerable challenge to standard numerical schemes due to the discontinuity of the material parameters. The standard schemes locate the horizontal interface half-way between the grid lines. This results in the apparent position of the interface to be below or above its actual position resulting in the late or early arrivals of the reflected waves respectively. This is evidently manifested in the reflected waves for the standard algorithm. Our modified algorithm senses the correct location of the interface, hence a better agreement of the reflected signals with the semi-analytical solutions.

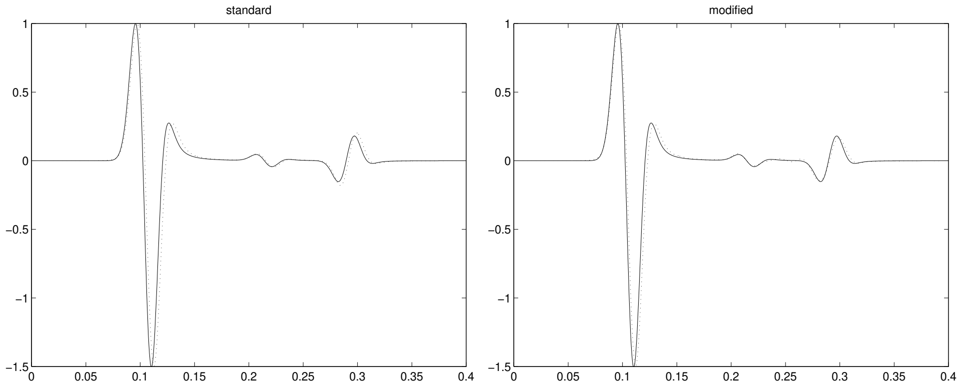

Figure 4: *Horizontal Displacement signals in receiver 1.*

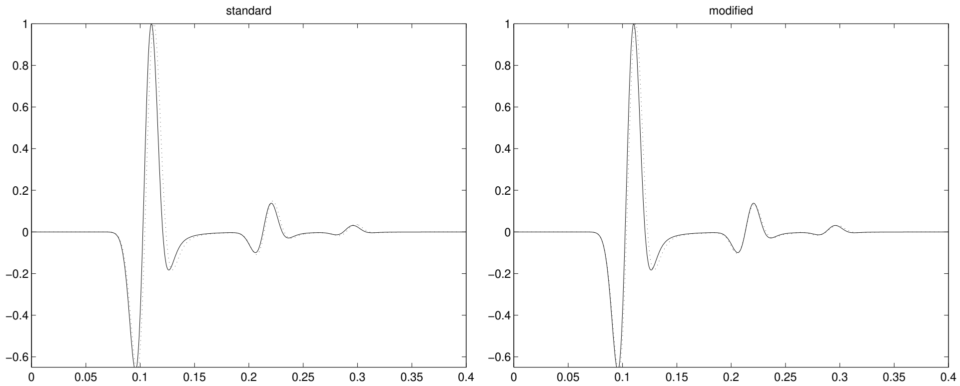

Figure 5: *Vertical Displacement signals in receiver 1.*

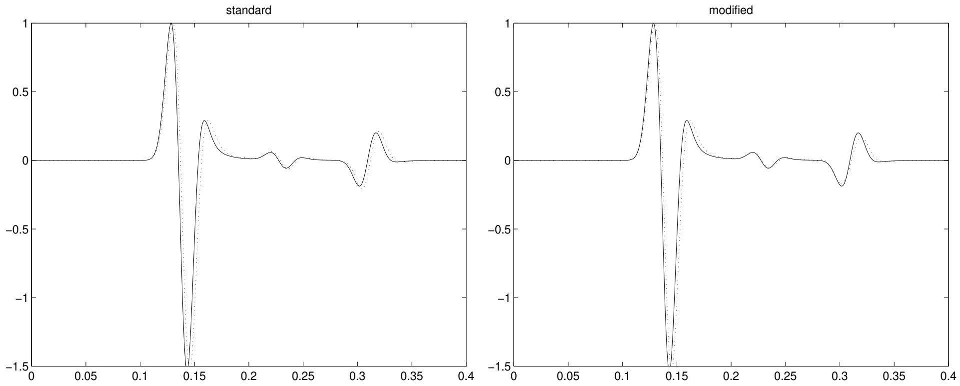

Figure 6: *Horizontal Displacement signals in receiver 2.*

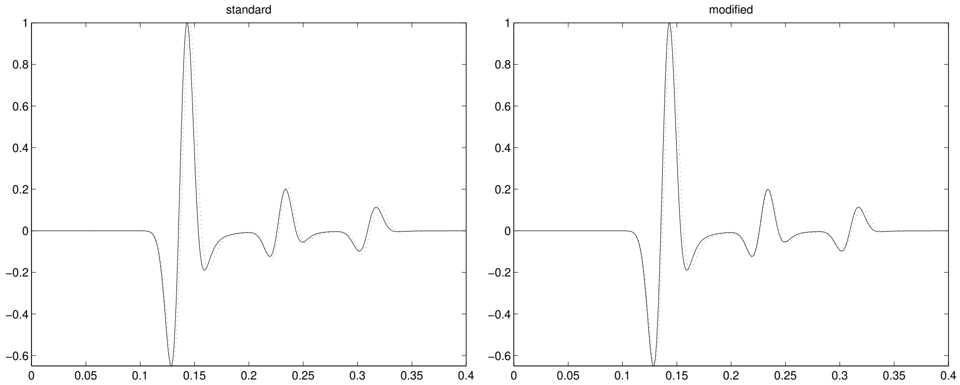

Figure 7: *Vertical Displacement signals in receiver 2.*

5.2 Plane Dipping Interface

This example models two elastic half-spaces with a plane dipping interface. The model configuration is as shown in fig. (8). The dipping angle is 11.1^o, hence way out of alignment with the grid lines. Consequently, the staircase representation of the interface is pronounced. The receivers are placed parallel to the dipping interface.

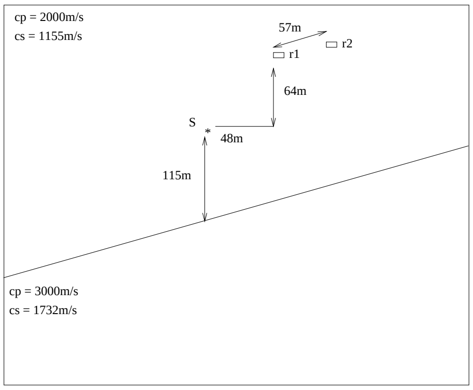

Figure 8: *Configuration of dipping interface model. (S) source, (r1, r2) receivers*

Figures 9 - 12 show displacement time series at the two receivers. The standard and modified schemes are compared to the semi-analytic solutions. Grid diffractions are clearly seen as spurious oscillations at the tail end of the propagation. Our modified scheme is observed to dampen these oscillations considerably.

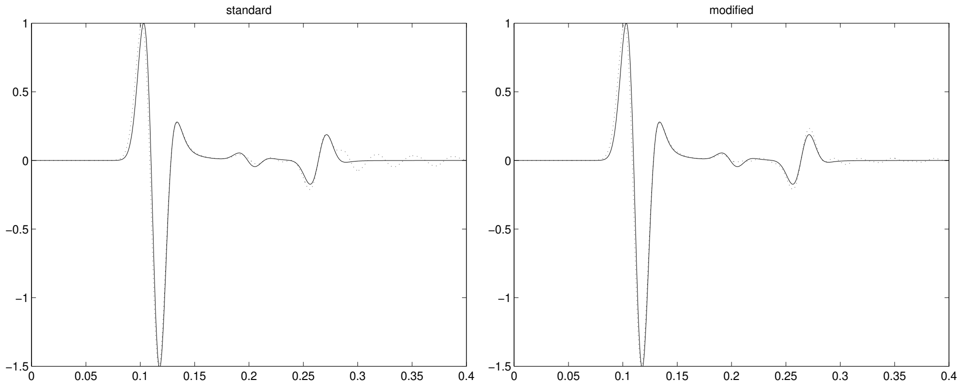

Figure 9: *Horizontal displacement time series for receiver 1. Plane Dipping interface angle* 11.1^o.

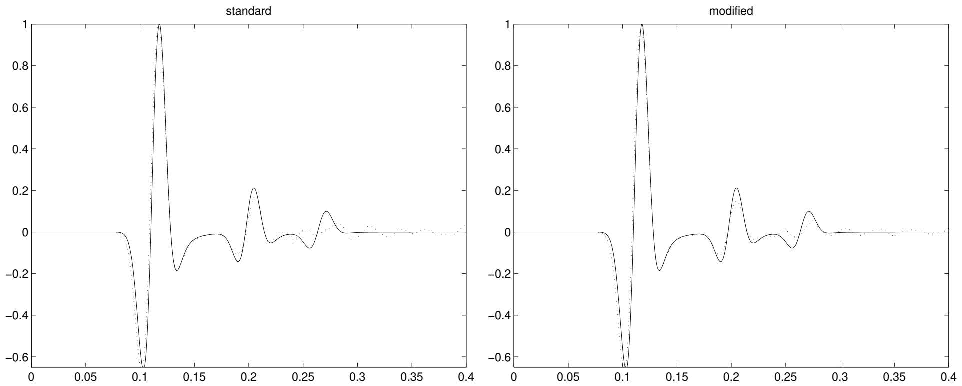

Figure 10: *Vertical displacement time series for receiver 1. Plane Dipping interface angle* 11.1^o.

Perhaps a better picture of the dampening of spurious wave fronts is better manifested in the snapshot of the shear wavefield, (eq. (11)) taken at $t = 300msec$, see fig. 13. Diffractions are of larger concern for S-waves than for P-waves since P-waves have higher propagating velocities and are thus better resolved on the computational grid.

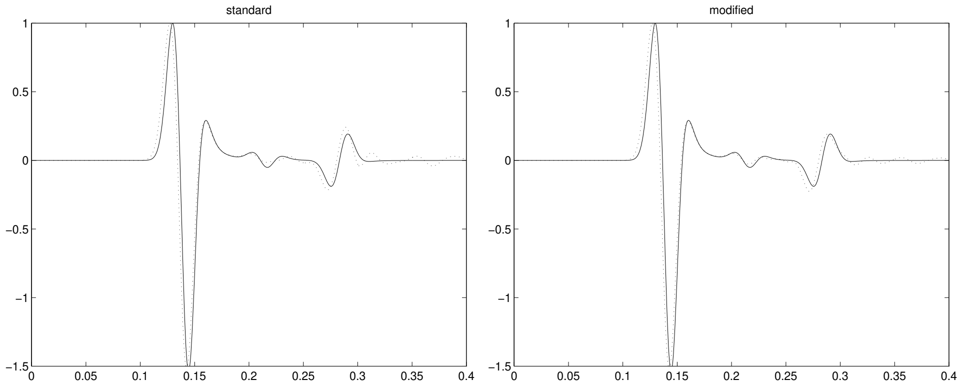

Figure 11: *Horizontal displacement time series for receiver 2. Plane Dipping interface angle* 11.1^o.

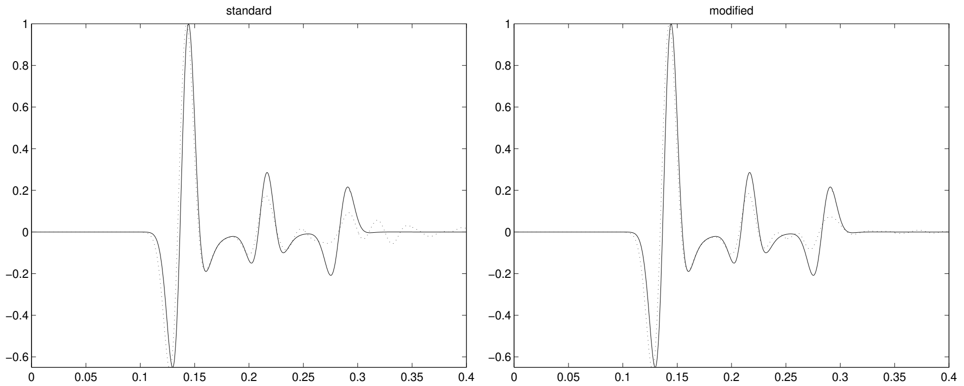

Figure 12: *Vertical displacement time series for receiver 2. Plane Dipping interface angle* 11.1^o.

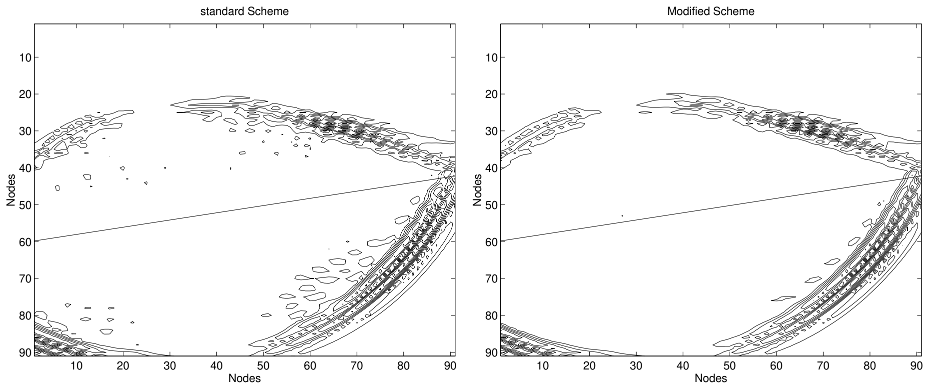

Figure 13: *Snapshot of the rotational part of the wave field, S, at* $t = 300msec$

6 Conclusion

We have presented a new modification scheme to the standard differentiation operator in forward modeling of elastic seismic waves in 2D discontinuous media. This new scheme ensures uniform convergence, hence reduces Gibbs oscillations. It is applicable to virtually any differentiation scheme.

Results from horizontal and dipping interface models using pseudospectral algorithm were compared with semi-analytical solutions obtained by ray-tracing technique. More accurate results are obtained with our modified scheme than with the standard scheme. In the tests, second order center difference scheme were used. We believe that a combination of this scheme with higher order time integration schemes, like the spectrally accurate scheme proposed by Tal Ezer will produce even better results. Another advantage of this scheme is that it is time independent, hence the correction factors are pre-computed. The difference, therefore, between the complexity of the modified and standard algorithms is marginal.

References

[1] O. Holberg, "Computational aspects of the choice of operator and sampling interval for numerical differentiation in large-scale simulation of wave phenomena", *Geophysical Prospecting* , **35** (1987), 629–655.

[2] P. Sqazzero, M. Kindelan & A. Kamel, "Dispersion-bounded numerical integration of the elasto-dynamic equations with cost-effective staggered schemes", *Computer Methods in Applied Mechanics and Engineering* , **80** (1990), 165–172.

[3] P. Mora, "The seismic simulation project", *Technical Report - 5th periodical report. , Institut Physique du Globe Paris* , (1993).

[4] E. Priolo & G. Seriani, "Advancements in large scale seismic wave modeling by the finite element method", *In Abstracts, 55th Meeting of the European Association for Exploration Geophysicists, Stavanger, Norway* , (1993).

[5] P. Berg, "On Forward Modeling of Seismic Waves for Exploration of Oil and Natural Gas", *PhD thesis, Technical University of Denmark, The Danish Center for Applied Mathematics and Mechanics, Report No. S. 50* , (1989).

[6] P. Berg, F. If & O. Skovgaard, "A spectral method for seismic wave propagation in elastic media", *Wave Motion* , **12** (1990), 415–427.

[7] M. Resheff, D. Kosloff, M. Edwards & C. Hsiung, "Three-dimensional elastic modeling by the Fourier method", *Geophysics* , **53** (1990), 1184–1193.

[8] D. Kosloff, D. Kessler, A. Q. Filho, E. Tessmer, A. Behle & R. Strahilevitz, "Solution of the equations of dynamic elasticity by a chebyshev spectral method", *Geophysics* , **55** (1990), 734–748.

[9] C. Filho, "Elastic modeling and migration in elastic models", *PhD thesis, Standford university* , (1992).

[10] B. Fornberg, "The pseudospectral method: accurate representation of interfaces in elastic wave equations", *Geophysics* , **53** (1988), 625–627.

[11] F. Muir, J. Dellinger, J. Etgen & D. Nichols, "Short note: Modeling elastic fields across irregular boundaries", *Geophysics* , **57** (1992), 1189–1193.

[12] J. D. Achenbach, "Wave propagation in elastic solids", *North Holland, Amsterdam* , (1973).

[13] C. Cerjan, D. Kosloff, R. Kosloff & M. Reshef, "Short note: A nonreflecting boundary condition for discrete acoustic and elastic wave equations", *Geophysics* , **50** (1985), 705–708.

[14] H. Tal-Ezer, "Spectral methods in time for hyperbolic equations", *SIAM J. Numerical Analysis* , **23** (1986), 11–26.

[15] D. Kosloff & E. Baysal, "Forward modeling by a fourier method", *Geophysics* , **57** (1982), 1402–1412.

[16] A. M. Skånøy, "Finite difference modeling of elastic waves on parallel computers", *Master's thesis, Dept. of Informatics, University of Bergen, Norway* , (1993).

[17] H. Munthe-Kaas & A. M. Skånøy, "Modelling Waves in Discontinuous Media - Uniformly Converging Schemes", *In Abstracts, 55th Meeting of the European Association for Exploration Geophysicists, Stavanger, Norway* , (1993).